Received: 23 January 2020 | Accepted: 15 February 2020

DOI: 10.1111/gcbb.12682

ORIGINAL RESEARCH

GLOBAL CHANGE BIOLOGY BIOENERGY WILEY

Including albedo in time-dependent LCA of bioenergy

Petra Sieber | **Niclas Ericsson** | **Torun Hammar** | **Per-Anders Hansson**

Department of Energy and Technology, Swedish University of Agricultural Sciences (SLU), Uppsala, Sweden

Correspondence
Petra Sieber, Department of Energy and Technology, Swedish University of Agricultural Sciences (SLU), Uppsala SE750 07, Sweden.
Email: petra.sieber@slu.se

Funding information
Swedish Government

Abstract

Albedo change during feedstock production can substantially alter the life cycle climate impact of bioenergy. Life cycle assessment (LCA) studies have compared the effects of albedo and greenhouse gases (GHGs) based on global warming potential (GWP). However, using GWP leads to unequal weighting of climate forcers that act on different timescales. In this study, albedo was included in the time-dependent LCA, which accounts for the timing of emissions and their impacts. We employed field-measured albedo and life cycle emissions data along with time-dependent models of radiative transfer, biogenic carbon fluxes and nitrous oxide emissions from soil. Climate impacts were expressed as global mean surface temperature change over time (ΔT) and as GWP. The bioenergy system analysed was heat and power production from short-rotation willow grown on former fallow land in Sweden. We found a net cooling effect in terms of ΔT per hectare (-3.8×10^{-11} K in year 100) and GWP_{100} per MJ fuel (-12.2 g CO_2e), as a result of soil carbon sequestration via high inputs of carbon from willow roots and litter. Albedo was higher under willow than fallow, contributing to the cooling effect and accounting for 34% of GWP_{100}, 36% of ΔT in year 50 and 6% of ΔT in year 100. Albedo dominated the short-term temperature response (10–20 years) but became, in relative terms, less important over time, owing to accumulation of soil carbon under sustained production and the longer perturbation lifetime of GHGs. The timing of impacts was explicit with ΔT, which improves the relevance of LCA results to climate targets. Our method can be used to quantify the first-order radiative effect of albedo change on the global climate and relate it to the climate impact of GHG emissions in LCA of bioenergy, alternative energy sources or land uses.

KEYWORDS

albedo, bioenergy, climate impact, greenhouse gases, land use change, LCA, life cycle assessment, willow

1 | INTRODUCTION

Biomass as a source of renewable energy can decrease dependency on fossil fuels and contribute to climate change mitigation by storing carbon in biomass and soil (Creutzig et al., 2015). For bioenergy to generate negative carbon emissions, more carbon has to be sequestered during feedstock production than is released along the life cycle (Searchinger et al., 2008; Tilman, Hill, & Lehman, 2006). The greenhouse gas (GHG) balance of bioenergy is

commonly determined using life cycle assessment (LCA), a standardized method for evaluating potential environmental impacts (Cherubini et al., 2009; Creutzig et al., 2015; Hellweg & Milà i Canals, 2014). All direct and indirect sources of GHG emissions need to be considered, including production of inputs, field operations, land use, transport, processing and energy conversion.

Land management and land use change (direct or indirect) can dominate the GHG balance of bioenergy systems due to changes in carbon stocks (Searchinger et al., 2008) and nitrous oxide emissions from nitrogen application (Cherubini et al., 2009). Compared to annual crops, perennial grasses and short-rotation coppice (SRC) species are associated with lower land-related emissions as they require less fertilization and have the potential to sequester additional carbon in soil (Don et al., 2012). Cultivation of perennial crops on marginal lands has been suggested to minimize competition with other agricultural uses and increase the potential for soil carbon sequestration (Gelfand et al., 2013; Whitaker et al., 2018).

Land use further affects the climate by modifying the biophysical properties of the land surface, including albedo, evapotranspiration efficiency and surface roughness (Pielke et al., 2002). These properties regulate fluxes of energy, water and momentum between the surface and the atmosphere and influence climate variables on local, regional and global scale (Pielke et al., 1998). Albedo, the share of solar flux reflected back from the ground, directly impacts the Earth's energy budget. The more reflective a surface, the higher its albedo and the greater the potential for radiative cooling and eventually temperature change. Through this mechanism, land use over time has led to substantial radiative cooling (Betts, Falloon, Goldewijk, & Ramankutty, 2007; Ghimire et al., 2014) and resulted in lower temperatures (Betts et al., 2007). This is because most historical land cover change to date has been agricultural expansion in temperate regions, where the shift from forests to more reflective croplands has increased albedo and primarily caused albedo-related cooling (Betts et al., 2007). There is concern that albedo change today could offset the cooling achieved by emissions reduction measures that affect surface properties, such as afforestation (Arora & Montenegro, 2011), biomass plantation (Schaeffer et al., 2006) and biochar application (Smith, 2016). It has also been suggested that land could be managed proactively towards higher albedo to mitigate global warming, for example, by introducing cover crops (Carrer, Pique, Ferlicoq, Ceamanos, & Ceschia, 2018) or by using reflective materials on urban surfaces (Akbari, Menon, & Rosenfeld, 2009).

Albedo can be an important contributor to the life cycle climate impact of bioenergy. LCA studies show that changes in albedo may cause radiative forcing (RF) of similar magnitude to the RF of net GHG emissions in a bioenergy system (Cai et al., 2016; Caiazzo et al., 2014; Cherubini, Bright, & Stromman, 2012). However, the importance of albedo depends on a range of case-specific factors such as local climate, insolation, soil type, vegetation, management and yield. Therefore, additional research is needed to understand when, where and at which scale surface albedo should be considered in the planning and assessment of bioenergy systems.

The relative importance of albedo for the life cycle climate impact depends on the time perspective chosen for the assessment. Albedo change leads to RF that persists only as long as surface properties are modified, while the RF of GHGs decays gradually after emission and may persist for decades or centuries. Metrics commonly used in LCA, such as global warming potential (GWP), are calculated for a single time horizon. This results in unequal weighting of short-term and long-term climate forcers, which may be inappropriate in joint assessments of well-mixed GHGs, short-lived climate forcers and albedo effects (Peters, Aamaas, Lund, Solli, & Fuglestvedt, 2011; Tanaka, Peters, & Fuglestvedt, 2010). Methods have been developed to express climate impacts as a function of time (Levasseur et al., 2016), based on annual emission inventories and metrics such as instantaneous RF (Levasseur, Lesage, Margni, & Samson, 2013; Pourhashem, Adler, & Spatari, 2016), cumulative RF (Levasseur et al., 2013) or global mean surface temperature change (Ericsson et al., 2013). These time-dependent LCA methods have been used to compare the impact of GHGs with different lifetimes, account for the timing of emissions and include temporary storage of biogenic carbon. To our knowledge, few LCA studies have applied time-dependent methods to albedo using RF as a metric (Bright, Stromman, & Peters, 2011; Cherubini et al., 2012; Jørgensen, Cherubini, & Michelsen, 2014), whereas the majority has used GWP (Arvesen et al., 2018; Cai et al., 2016; Caiazzo et al., 2014; Meyer, Bright, Fischer, Schulz, & Glaser, 2012).

The aim of this study was to improve understanding of how albedo affects the life cycle climate impact of bioenergy. Specific objectives were (a) to include albedo in time-dependent LCA; and (b) to evaluate the magnitude of the life cycle climate impact due to albedo change and compare it with carbon sequestration and GHG emissions in a bioenergy system. For this purpose, LCA methodology was combined with time-dependent models of the production chain, biogenic carbon fluxes, nitrous oxide emissions from soil and radiative transfer. Climate impacts were expressed as global mean surface temperature change, which is a function of time, and as GWP using a 100 year time horizon.

The system analysed was production of heat and power from SRC willow cultivated on former long-term fallow land for 50 years. The study site was located in Västra Götaland County in south-western Sweden (58.2667, 12.7667). About 8% (36,000 ha) of the county's arable land area was under fallow between 2015 and 2019 (Swedish Board of Agriculture, 2019), whereof more than half was fallow for 3 years or

longer (Statistics Sweden, 2017). Hence, there is potential to cultivate perennial energy crops with a low risk of displacing food or feed production. Willow is a perennial energy crop that can provide rapid growth and high yields at low levels of agronomic inputs and management. Studies have shown good potential of SRC willow bioenergy systems to generate low (Heller, Keoleian, & Volk, 2003) or negative emissions (Ericsson et al., 2013; Hammar, Hansson, & Sundberg, 2017; Hillier et al., 2009).

2 | MATERIALS AND METHODS

2.1 | Goal and scope of the LCA

Life cycle assessment was used to analyse cultivation of SRC willow on former fallow in south-western Sweden for 50 years, supplying wood chips to a local energy plant for combined heat and power (CHP) production. The goal was to determine the climate impact of SRC willow bioenergy, including the three major GHGs (carbon dioxide [CO_2], methane [CH_4], and nitrous oxide [N_2O]) and albedo. Results are presented per hectare of land and per MJ fuel energy content, based on the lower heating value (LHV).

The willow scenario included production of inputs, field operations, transport and combustion of wood chips (Figure 1). Transformation and distribution losses of heat and electricity were not included. Direct effects of land use were accounted for, comprising the initial transformation of fallow land and the change in occupation during 50 years of willow production. The production period consisted of two consecutive 25-year rotations of SRC willow. Each rotation started with soil preparation in autumn and establishment of a new plantation in the following spring. The rotation then consisted of eight 3-year cutting cycles, followed by one fallow year between termination of the old plantation and establishment of a new plantation. The crop was assumed to be harvested in spring every third year, yielding 20 Mg DM/ha in the first cutting cycle of each rotation and 30 Mg DM/ha in cutting cycles 2–8 (Hollsten, Arkelöv, & Ingelman, 2013).

The reference scenario included natural gas as a fuel combusted in the CHP plant. The land remained fallow for the duration of the study period, resulting in no transformation or change in occupation. Fallow was defined as set-aside land vegetated by grass with annual productivity of 3 Mg DM/ha. The management of green fallow was identical in the reference scenario and before the study period (i.e. when fallow was the former land use).

Time-dependent LCA methodology (Ericsson et al., 2013) was used to quantify the climate impact due to annual GHG emissions and albedo changes. Emissions of CO_2, CH_4 and N_2O were recorded for each year of the study period, in a time-distributed life cycle inventory. Upstream emissions from production of inputs were assigned to the year in which the inputs were used. CO_2 from the decay of methane was recorded as an emission in the year following the decay. Changes in annual carbon stocks were recorded as positive or negative CO_2 emissions. Surface albedo change was converted to the corresponding change in shortwave fluxes at the top of the atmosphere (TOA) and recorded in the inventory

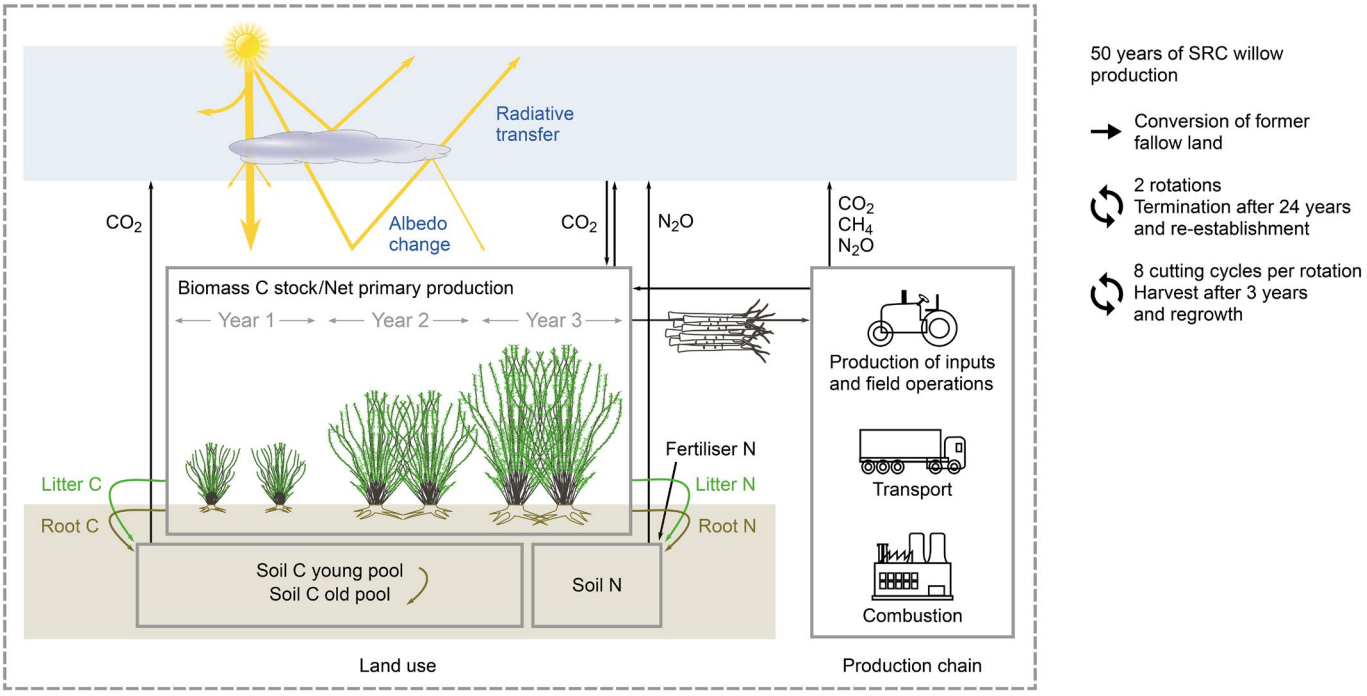

FIGURE 1 System components and life cycle inventory flows in the willow scenario. SRC, short-rotation coppice

as annual mean RF. Climate impacts were assessed as global mean surface temperature change over time up to year 100, and as CO_2-equivalents using GWP_{100}.

2.2 | Production chain

In the willow scenario, the production chain (production of inputs, field operations, transport and combustion) was based on Hammar, Ericsson, Sundberg, and Hansson (2014), using data from previous studies of SRC willow in Sweden. Data and references for activities, inputs and emissions are provided in Tables S1–S3. Management operations in the establishment phase included soil preparation by ploughing and harrowing, chemical and mechanical weed control, and planting of willow seedlings. Fertilizer was applied repeatedly during the rotation, following recommendations for the expected yield and net primary production (NPP; Aronsson, Rosenqvist, & Dimitriou, 2014; Börjesson, 2006). Harvesting using direct chipping, field transport and road transport took place in the third year of each cutting cycle. After the last harvest in each rotation, the plantation was terminated by mechanical destruction of plant residues and rootstocks.

The wood chips were transported 40 km to the CHP plant. Storage losses were considered assuming 3% dry matter loss during an average storage period of 60 days (Elinder, Almquist, & Jirjis, 1995). An LHV of 15.8 MJ/kg DM was used for the willow fuel (Hammar et al., 2017). Combustion emissions of N_2O and CH_4 were calculated based on the LHV (Table S2). Remaining fuel carbon that was not emitted as CH_4 was converted to CO_2 and considered under biogenic carbon fluxes.

In the reference scenario, the usage of natural gas was equivalent to the amount of willow fuel supplied per year in terms of the LHV. Emissions from production, distribution and combustion were calculated based on the LHV (Table S2). Green fallow was cut every autumn to avoid the growth of shrubs. Biomass was left in the field to decompose, providing input to the soil carbon pool. Activity data and emissions are presented in Table S4.

2.3 | Biogenic carbon fluxes

Carbon stocks in living biomass and soil were determined for each year and used to calculate annual net carbon fluxes to the atmosphere. Carbon in biomass was modelled based on annual NPP in different plant compartments (Tables S5 and S6). Willow stem NPP was calculated according to expected yield per cutting cycle and growth rates of 25%, 40% and 35%, respectively, in years 1, 2 and 3 of each cutting cycle (Ericsson et al., 2013). Quantities of willow leaves, fine roots and coarse roots were derived from NPP allocation in willow relative to stem growth (Rytter, 2001). Fallow NPP was based on annual productivity. Quantities of fallow fine roots and coarse roots were calculated based on carbon allocation in grassland (Bolinder, Janzen, Gregorich, Angers, & VandenBygaart, 2007).

A carbon content of 50% DM was assumed for willow stems and coarse roots (including stumps) and 45% DM for willow leaves and fine roots and for fallow grass leaves, fine roots and coarse roots (Table S7). Willow stems accumulated carbon until harvest and combustion after 3 years. Coarse roots accumulated under continued production until the willow plantation was terminated or the fallow was discontinued. Fine roots (including root exudates), willow litter and fallow grass leaves were recorded as annual turnover. The carbon in different crop residue fractions, that is, willow litter and roots, and fallow grass leaves and roots, was recorded as input to the soil pool in the year following the biomass stock change.

Carbon in soil was modelled using ICBMr, a version of the Introductory Carbon Balance Model (Andrén & Kätterer, 1997) adapted for use of annual inputs per production region, soil type and crop type (Andrén, Kätterer, & Karlsson, 2004). The model consists of two carbon pools, young (Y) for fresh organic matter and old (O) for stabilized material. Annual carbon inputs (i) enter Y and are transferred to O according to the humification coefficient (h), defining the substrate fraction stabilized. This fraction is about 2.3-fold higher for root-derived carbon than for litter and other above-ground crop residues (Kätterer, Bolinder, Andrén, Kirchmann, & Menichetti, 2011). Therefore, above-ground and below-ground carbon were modelled separately as inputs i_a and i_b, with humification coefficient h_a and h_b respectively (Ericsson et al., 2013; Table S8). Carbon in the young and old pools was calculated using Equations (1) and (2), respectively, and annual time steps:

$$Y_{[a,b]}[t] = \left(Y_{[a,b]_{t-1}} + i_{[a,b]_{t-1}}\right) \exp^{-k_Y r_e}, \tag{1}$$

$$O[t] = \left(O_{t-1} - \left(\frac{h_a k_Y}{k_O - k_Y}\left(Y_{a_{t-1}} + i_{a_{t-1}}\right) + \frac{h_b k_Y}{k_O - k_Y}\left(Y_{b_{t-1}} + i_{b_{t-1}}\right)\right)\right) \exp^{-k_O r_e} + \left(\frac{h_a k_Y}{k_O - k_Y}\left(Y_{a_{t-1}} + i_{a_{t-1}}\right) + \frac{h_b k_Y}{k_O - k_Y}\left(Y_{b_{t-1}} + i_{b_{t-1}}\right)\right) \exp^{-k_Y r_e}, \tag{2}$$

where k_Y and k_O are decomposition constants per pool and r_e is an external decomposition control affecting carbon losses from both pools. The external factor accounts for the effect of soil temperature, soil water content and degree of cultivation on decomposer activity (Andrén et al., 2004). A value of 0.95 and 1.03 was calculated for willow and green fallow, respectively, accounting for climate and soil types in Västra Götaland, crop type, and management intensity and frequency.

Soil carbon stocks were assumed to be in equilibrium under the long-term fallow preceding the willow. This means that annual inputs and losses were equal, resulting in constant stocks. Equilibrium values for Y_a, Y_b and O were computed through a 1,000 year spin-up simulation and used as starting values in year 0 when running ICBMr for willow and fallow respectively (see Table S8). Total soil carbon per year was calculated as the sum of the pools, that is, $C_{soil}[t] = Y_a[t] + Y_b[t] + O[t]$.

2.4 | Nitrous oxide emissions from soil

Microbial activity leads to formation of N_2O from nitrogen added with synthetic fertilizer or present in above-ground and below-ground crop residues (Table S9). Three emissions pathways were considered for synthetic and biogenic nitrogen inputs to soil: (1) direct N_2O emissions; (2) indirect N_2O emissions following volatilization and subsequent redeposition; and (3) indirect N_2O emissions following leaching and runoff.

Emissions were calculated following the IPCC Guidelines for National Greenhouse Gas Inventories, using disaggregated values from the 2019 refinement (IPCC, 2019). Volatilization of nitrogen in above-ground crop residues is not included in the IPCC default values. Therefore, a volatilization factor (f) was calculated based on nitrogen content (N_{bio}, g/kg DM) in litter and grass leaves respectively (de Ruijter & Huijsmans, 2012; Equation 3). Emissions factors are summarized in Table S10.

$$f = 0.4 \times N_{bio} - 5.08. \quad (3)$$

2.5 | Surface albedo and radiative transfer

Downwelling and reflected shortwave irradiance were measured with pyranometer pairs (Hukseflux NR-1, 285–3,000 nm) at two sites in south-western Sweden. Measurements from April 2013 to March 2016 covered a full 3-year cutting cycle of SRC willow (*Salix viminalis* L.). A nearby mire vegetated by grasses and sedges was used as a proxy for long-term fallow. Irradiance was sampled at 30 min intervals and processed according to Sieber, Ericsson, and Hansson (2019) to obtain corrected and gap-filled time series.

Albedo change increases or decreases the solar flux leaving the Earth's surface. The radiation is absorbed and scattered by clouds, aerosols and gases on its way to the top of the atmosphere (TOA), where a change in the upwelling shortwave flux eventually causes RF. Upwelling irradiance at the TOA in W/m^2 is given by (Winton, 2005):

$$R_{TOA\uparrow} = R_{TOA\downarrow} \frac{\tau_\downarrow \tau_\uparrow}{1 - \alpha r_\uparrow} \alpha, \quad (4)$$

where τ is transmittance during a single downward or upward pass through the atmosphere. The denominator represents an infinite number of reflections between the surface with albedo α and the atmosphere with reflectivity r. RF from albedo change (RF_α, W/m^2) can then be expressed using the partial derivative of Equation (4) in relation to α (Equation 5; Bright & O'Halloran, 2019). The effect of multiple reflection, which increases solar irradiance at surfaces with higher albedo and reinforces RF_α, is thereby included:

$$RF_\alpha = -\frac{\partial R_{TOA\uparrow}}{\partial \alpha} \Delta\alpha = -R_{TOA\downarrow} \frac{\tau_\downarrow \tau_\uparrow}{(1 - \alpha r_\uparrow)^2} \Delta\alpha. \quad (5)$$

A single atmospheric layer with isotropic properties was assumed to simplify radiative transfer (Stephens et al., 2015). By taking τ and r as directionally independent, atmospheric transmittance and reflectivity can be calculated from four shortwave fluxes according to Equations (6) and (7) (Winton, 2005):

$$\tau = \frac{R_{TOA\downarrow} R_{S\downarrow} - R_{TOA\uparrow} R_{S\uparrow}}{R_{TOA\downarrow}^2 - R_{S\uparrow}^2}, \quad (6)$$

$$r = \frac{R_{TOA\downarrow} R_{TOA\uparrow} - R_{S\downarrow} R_{S\uparrow}}{R_{TOA\downarrow}^2 - R_{S\uparrow}^2}, \quad (7)$$

where $R_{TOA\uparrow}$ and $R_{TOA\downarrow}$ are upwelling and downwelling irradiance at the TOA and $R_{S\uparrow}$ and $R_{S\downarrow}$ are upwelling and downwelling irradiance at the surface. Here we used variables from the ERA5 global reanalysis dataset at a resolution of 31 km and 1 hr (Copernicus Climate Change Service [C3S], 2017). The data were averaged across 15 years (2004–2018) to generate standard atmospheric conditions, which were used in all years of the study period.

Using Equations (6)–(8), annual mean albedo RF can be calculated for each year of the study period and recorded as inventory vector $I_\alpha[t]$:

$$I_\alpha[t] = \frac{A}{A_E} \frac{1}{N} \sum_{s=1}^{N} -R_{TOA\downarrow t,s} \frac{\tau_{t,s}^2}{(1 - \alpha_{t,s} r_{t,s})^2} \Delta\alpha_{t,s}, \quad (8)$$

where A is the affected area in relation to the Earth's total surface area ($A_E = 5.1 \times 10^{14}$ m^2) and N is the number of sub-annual time steps s. The time step has to be chosen sufficiently small to account for the seasonal covariation of albedo change with irradiance (Bright, Zhao, Jackson, & Cherubini, 2015) and radiative transfer (Sieber et al., 2019). Here surface and atmospheric properties (α, τ, r) were calculated from 5-day-average irradiances to smoothen variability in the temporally decoupled data sets (i.e. measured albedo from 2013 to 2016 and climatological shortwave fluxes from 2004 to 2018). This is in contrast

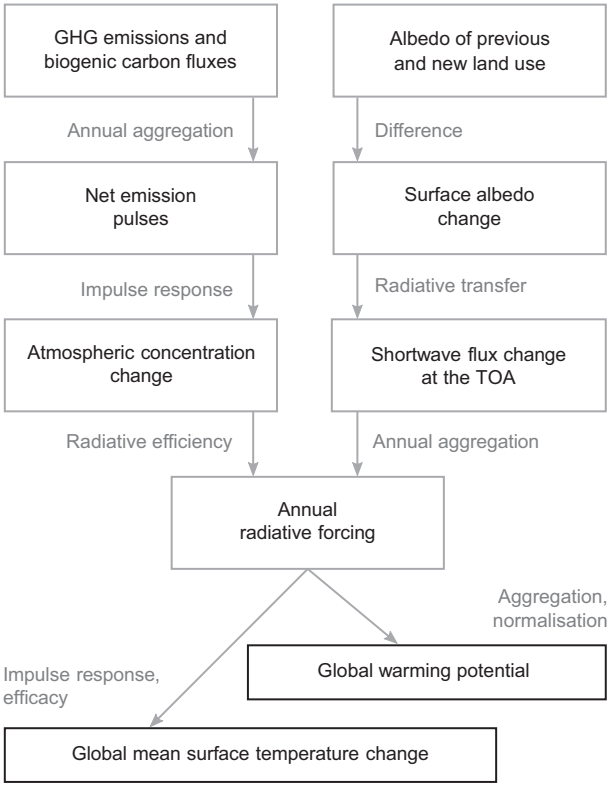

FIGURE 2 Modelling steps from input data for greenhouse gases (GHGs) and albedo to climate impact using time-dependent life cycle assessment methodology. TOA, top of the atmosphere

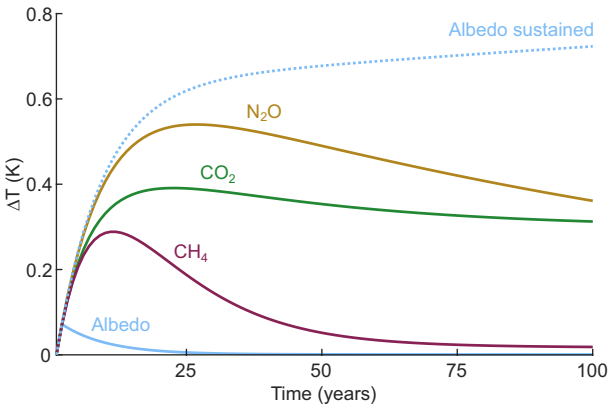

FIGURE 3 Annual temperature response to radiative forcing of 1 W/m^2 in year 0, resulting from emission pulses of 570 Pg CO_2, 2.8 Pg N_2O or 4.7 Pg fossil CH_4 in year 0; from temporary albedo change in year 0; or from sustained albedo change in years 0–100. Metric values taken from Myhre et al. (2013)

to Sieber et al. (2019), who matched hourly albedo change, irradiance and radiative transfer during the same 3 years.

2.6 | Climate impact assessment

The time-dependent characterization model was taken from the methodology for GHGs in Ericsson et al. (2013) and expanded for albedo (Figure 2). Annual GHG emissions and albedo RF were converted to global mean surface temperature change (ΔT). Impacts were expressed as a function of time from the start of the study period up to year 100. Including the timing of impacts can better reflect the relative contribution of climate forcers with different perturbation lifetimes (Aamaas, Peters, & Fuglestvedt, 2013; Boucher & Reddy, 2008). Perturbation lifetimes of climate forcers included in this study range from instantaneous for albedo change up to centuries for CO_2. Implications for the temperature response are illustrated in Figure 3.

The time-dependent characterization model can be written as a convolution sum (here square brackets denote discrete vectors, whereas round brackets denote continuous functions):

$$\Delta T_x[H] = \sum_{t=0}^{H} I_x[t]\mathrm{AGTP}_x[H - t], \quad (9)$$

where $I_x[t]$ in kg is a vector with annual inventory results for forcing agent x, and $\mathrm{AGTP}_x[t]$ is the absolute global temperature potential of x at the same time step. $\mathrm{AGTP}_x(t)$ in K/kg is defined as the change in global mean surface temperature over time, following a pulse release of x in year 0. By performing the convolution in Equation (9), $\Delta T_x[H]$ gives the response to emissions and forcings in different years up to evaluation time H.

The AGTP of GHGs is determined as the convolution integral of two impulse response functions (IRF; Boucher & Reddy, 2008; Fuglestvedt et al., 2010):

$$\mathrm{AGTP}_x(H) = e_x \int_{t=0}^{H} \mathrm{IRF}_x(t)\mathrm{IRF}_T(H - t)\mathrm{d}t, \quad (10)$$

where e_x is radiative efficiency of GHGs, that is, the additional RF per unit mass increase of gas x in the atmosphere, $\mathrm{IRF}_x(t)$ is the fraction of a gas remaining in the atmosphere after a pulse emission and $\mathrm{IRF}_T(t)$ is the temperature response of the climate system to a unit RF. Here we used $\mathrm{IRF}_x(t)$ for CO_2 based on the Bern Carbon Cycle Model (Joos et al., 2013), $\mathrm{IRF}_x(t)$ for CH_4 and N_2O based on simple exponential decay (Prather, 2007) and $\mathrm{IRF}_T(t)$ based on simulations with the HadCM3 climate model (Boucher & Reddy, 2008). The functions and metric values used are those summarized in the Supporting Information to the IPCC Fifth Assessment Report (Myhre et al., 2013).

Solving the convolution integral in Equation (10) and using the analytical solution of AGTP to calculate ΔT allows handling the characterization in LCA in discrete time steps according to Equation (9), without generating errors from numerical approximation (as it would happen if the convolution integral in Equation 10 was approximated by a convolution sum using discrete time steps). The analytical solution of AGTP is provided for CO_2, CH_4 and N_2O in Myhre et al. (2013).

Here we used the same approach for albedo and formulated $AGTP_\alpha(H)$ as the convolution integral of two IRFs, analogously to Equation (10). $IRF_\alpha(t)$ was written as a boxcar function that is 1 for $0 \le t < 1$. $IRF_T(t)$ is commonly used independently of the emitted species (Aamaas, Berntsen, Fuglestvedt, Shine, & Bellouin, 2016) and was therefore assumed identical with GHGs (Boucher & Reddy, 2008):

$$IRF_T(t) = \sum_{j=1}^{2} \frac{c_j}{d_j} \exp\left(\frac{-t}{d_j}\right), \quad (11)$$

where c_j are components of climate sensitivity and d_j a short and a long response timescale. The solution of AGTP for albedo RF was found by analytical integration and is given by (in $K\ (W\ m^{-2})^{-1}$):

$$AGTP_\alpha(H) = \sum_{j=1}^{2} c_j \left(\left(1 - \exp^{\frac{-H}{d_j}}\right) - \left(1 - \exp^{\frac{-(H-a)}{d_j}}\right) u(H-a)\right), \quad (12)$$

where the first exponential term is the response to a constant sustained forcing and the second one removes the response in $H \ge a$. The Heaviside step function $u(t)$ was defined to return 1 for $t \ge 0$ and 0 otherwise. Consequently, removal starts at a, which can be interpreted as the perturbation lifetime in years. For RF_α it corresponds to the aggregation interval chosen in the inventory, here $a = 1$. The same method can be used at any temporal resolution, for example, with a monthly inventory and $a = 1/12$. Combining Equations (9) and (12), the inventory vector of annual mean RF from albedo change, $I_\alpha[t]$, can be converted to $\Delta T_\alpha[H]$.

The metric values for c_j and d_j used in Equation (11) were derived from simulations with increased CO_2 concentration in a climate model with an equilibrium climate sensitivity of $\lambda_{CO_2} = \sum c_j = 1.06\ K\ (W\ m^{-2})^{-1}$ (Boucher & Reddy, 2008). Using the same parameters to model the response to albedo RF (Equation 12) assumes the same climate sensitivity and response timescales, despite differences in the vertical (surface vs. troposphere) and horizontal (global vs. local) distribution of the physical perturbation (Bright et al., 2015). Methods have been developed to account for differences in climate sensitivity by forcing agent (Hansen et al., 2005), which could be used to linearly scale $AGTP_\alpha(H)$. Here we assumed $\lambda_\alpha/\lambda_{CO_2} = 1$. Potentially lower or higher efficacy is addressed in Section 4.

Climate impacts were also assessed using GWP with a 100 year time horizon (GWP_{100}), a common climate metric in LCA. Characterization factors for GHGs including climate carbon cycle feedbacks were taken from Myhre et al. (2013). The corresponding characterization factor for annual mean albedo RF is $1/AGWP_{CO_2}(100) = 10.9 \times 10^{12}\ kg\ CO_2e\ (W\ m^{-2})^{-1}$, using $AGWP_{CO_2}(100) = 91.7 \times 10^{-15}\ W\ m^{-2}\ year\ kg^{-1}$ from Myhre et al. (2013). Consequently, the GWP_{100} of albedo RF can be calculated as:

$$GWP_\alpha^{100} = \frac{\sum_{t=0}^{100} I_\alpha[t]}{AGWP_{CO_2}^{100}}. \quad (13)$$

2.7 | Sensitivity analysis

A sensitivity analysis was performed to address uncertainty and variability associated with parameters, choices and the characterization model. The yields of SRC willow and fallow were reduced while keeping the original rates of fertilizer application. Soil carbon stocks were assumed to be lower than the equilibrium values in year 0. Potential feedback effects between yield and soil carbon were not considered. Fallow albedo was approximated using measured data for 2014 from an alternative site, a fresh clear-cut vegetated by grass in southern Sweden. Albedo RF calculated using Equation (8) was compared with that calculated using an alternative method (Ghimire et al., 2014; Sieber et al., 2019) based on monthly radiative kernels from global climate models (Table S13a).

3 | RESULTS

3.1 | Inventory analysis

The SRC willow plantation captured up to 18.7 Mg C/ha in biomass carbon stocks, with an average of 11.6 Mg C/ha during the study period (Figure 4a). Soil carbon stocks increased by 41.4 Mg C compared with the former fallow, which is equivalent to an average sequestration rate of 0.83 Mg C ha^{-1} $year^{-1}$ over 50 years. Nitrogen inputs varied with NPP and fertilization in each cutting cycle (Figure 4b). In the reference scenario, soil carbon stocks remained nearly stable at the equilibrium value of 57.9 Mg C/ha. Biomass carbon stocks did not change compared with the former land use (3.1 Mg C/ha). Nitrogen inputs were from biomass only and remained constant over the study period. Activity data and annual GHG emissions from the production chain can be found in Tables S2–S4.

In the willow scenario, annual albedo was elevated in every year of the cutting cycle (0.222, 0.215 and 0.212, compared with 0.165, 0.161 and 0.168 under fallow). On sub-annual timescales, 5 day albedo was mostly higher for willow than for fallow (Figure 5). Summer albedo increased by 0.05–0.1 under willow and led to peaks in negative RF between May and July. Winter albedo decreased by 0.3–0.6, because willow was less well covered by snow than fallow. However, the resulting positive RF was low as snowfall occurred only between November and March, when solar irradiance and atmospheric transmittance were low. Albedo RF in the willow scenario was $-5.3 \times 10^{-11}\ W/m^2$ on average during the study period, including one fallow year per rotation with no albedo

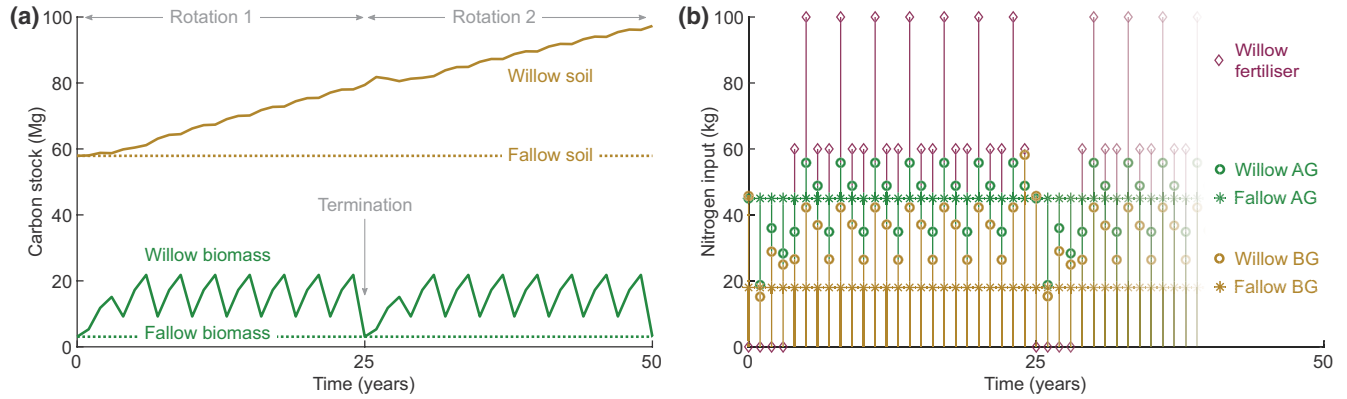

FIGURE 4 (a) Carbon stocks in biomass and soil and (b) annual nitrogen inputs from crop residues and mineral fertiliser, shown per hectare land use in the willow scenario (willow) and in the reference scenario (fallow) during the study period (50 years). Biomass includes all plant compartments; crop residues aboveground (AG) include willow leaves and fallow grass leaves; crop residues belowground (BG) include fine roots and coarse roots

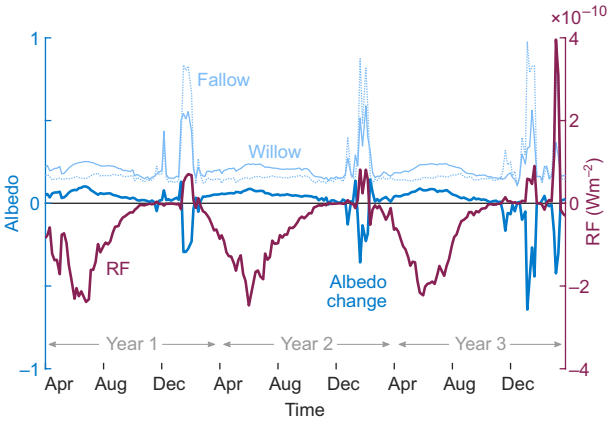

FIGURE 5 Willow albedo, fallow albedo and albedo change under willow relative to fallow (left axis) and radiative forcing (RF) from albedo change on 1 ha (right axis) during a 3-year cutting cycle of willow, using 5-day resolution

change (Table S11). Albedo did not change outside the study period or in the reference scenario.

Net inventory results for the entire study period are summarized in Table 1 and will be used to calculate GWP. Wood fuel produced during two rotations of SRC willow had a total energy content of 7,072 GJ/ha, corresponding to an annual average yield of 141 GJ/ha during the study period.

3.2 | Climate impact

The willow scenario had a net cooling effect on global mean surface temperature. The maximum effect, -10.1×10^{-11} K/ha, was reached at the end of the study period (year 50; Figure 6a). The main cooling resulted from increased soil carbon stocks under willow. Soil carbon sequestration alone was sufficient to offset positive emissions from the production chain (i.e. production of inputs, field operations, transport and combustion) and synthetic and biogenic N_2O from soil. Albedo change led to additional cooling, which was of similar magnitude to the warming effect of production emissions during the study period. The relative importance of albedo RF decreased over time as soil carbon accumulated under sustained production. After the study period, the temperature effect of albedo change was shorter than that of the GHGs, which remained in the atmosphere for decades to centuries (see Figure 3). Another consequence of CO_2 lifetime and gradual decay was that the sudden release of biomass carbon that had been sequestered throughout the production period led to 'overshoot warming' from year 60 onward.

The reference scenario had a warming effect over time, reaching a maximum of 38.4×10^{-11} K/ha in year 56 (Figure 6b). The main contributor was CO_2 from the use of natural gas as an alternative fuel. The reference land use led to a positive temperature response, mainly due to N_2O emissions from the application of biomass to soil.

Using GWP_{100} per MJ fuel energy content, the willow scenario had a climate impact of −12.2 g CO_2e (Table 2). Albedo was responsible for 34% of GWP_{100}, but only 6% of $\Delta T[100]$. The reference scenario had GWP_{100} of 81.9 g CO_2e/MJ fuel, which is of opposite sign and nearly sevenfold higher than that of the willow scenario. Natural gas was the single largest source of GHG emissions.

The differences between results with GWP_{100} and $\Delta T[100]$ stemmed from how the two climate metrics treat the timing of forcings (i.e. GHG emissions and albedo RF) and of impacts. The GWP metric applies the same time horizon to all forcings within the study period, whereas $\Delta T[H]$ applies the same evaluation time to all forcings, but a moving time horizon $H - t$ that becomes shorter the closer a forcing

	CO_2 (kg/ha)	CH_4 (kg/ha)	N_2O (kg/ha)	Albedo RF (10^{-9} W m^{-2} ha^{-1})
Willow scenario	−128,000	96.4	227	−2.65
Production chain	23,400	96.4	78.0	
Biomass carbon	0			
Soil carbon	−152,000			
Soil N_2O			149	
Albedo change				−2.65
Reference scenario	488,000	2,160	44.9	0
Production chain	875	0.380	0.000624	
Biomass carbon	0			
Soil carbon	0			
Soil N_2O			44.1	
Albedo change				0
Natural gas	487,000	2,160	0.782	

Abbreviation: RF, radiative forcing.

TABLE 1 Inventory results for the willow and reference scenarios aggregated over the study period, presented per system component and climate forcer. Production chain includes production of inputs, field operations, transport and combustion; biomass includes willow stems, leaves and roots and fallow grass leaves and roots; nitrous oxide emissions from soil (soil N_2O) include direct and indirect emissions due to addition of synthetic and biogenic nitrogen; albedo change refers to the difference between land use in the respective scenario and the former land use (i.e. fallow)

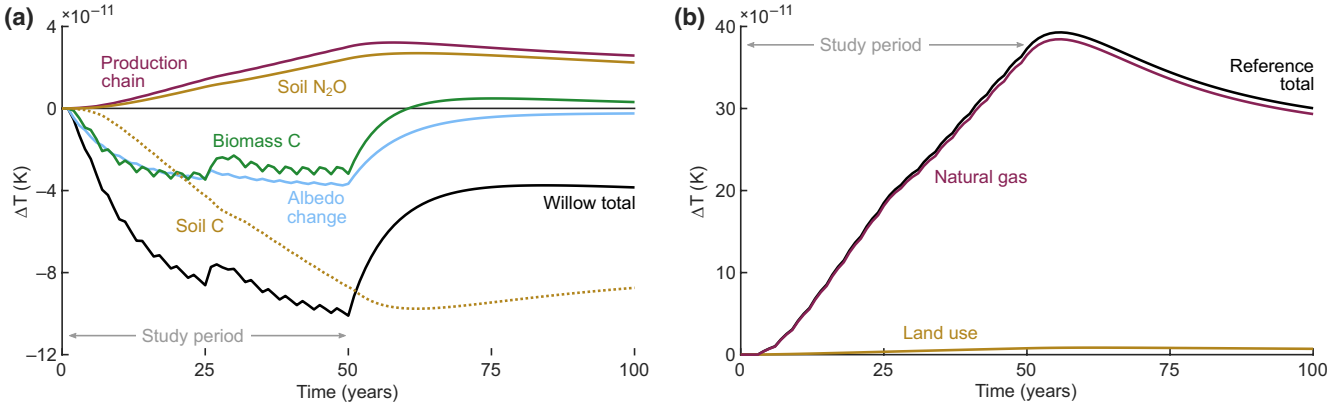

FIGURE 6 Climate impact of (a) the willow scenario and (b) the reference scenario expressed as global mean surface temperature change per hectare. Willow total includes albedo change and greenhouse gas (GHG) emissions from the production chain (production of inputs, field operations, transport and combustion), from carbon stock change in biomass (biomass C) and soil (soil C) and from addition of synthetic and biogenic nitrogen to soil (soil N_2O). Reference total includes GHG emissions from land use (production of inputs, field operations and soil N_2O) and from natural gas (production, distribution and combustion)

	GWP_{100} (g CO_2e/MJ)	ΔT[100] (10^{-11} K/ha)	ΔT[50] (10^{-11} K/ha)
Willow system	−12.2	−3.8	−10.1
Production chain	7.1	2.6	3.0
Biomass carbon	0	0.3	−3.2
Soil carbon	−21.5	−8.7	−8.7
Soil N_2O	6.3	2.2	2.4
Albedo change	−4.1 (34%)	−0.2 (6%)	−3.7 (36%)
Reference system	81.9	30.0	37.3
Land use	2.0	0.7	0.8
Natural gas	79.9	29.3	36.5

TABLE 2 Climate impact in the willow and reference scenarios using alternative functional units, metrics and evaluation times. The relative importance of albedo change in the willow scenario is highlighted. Land use emissions in the reference scenario (production chain and soil N_2O) are summarized. Results can be converted between functional units based on total energy production (7,072 GJ/ha)

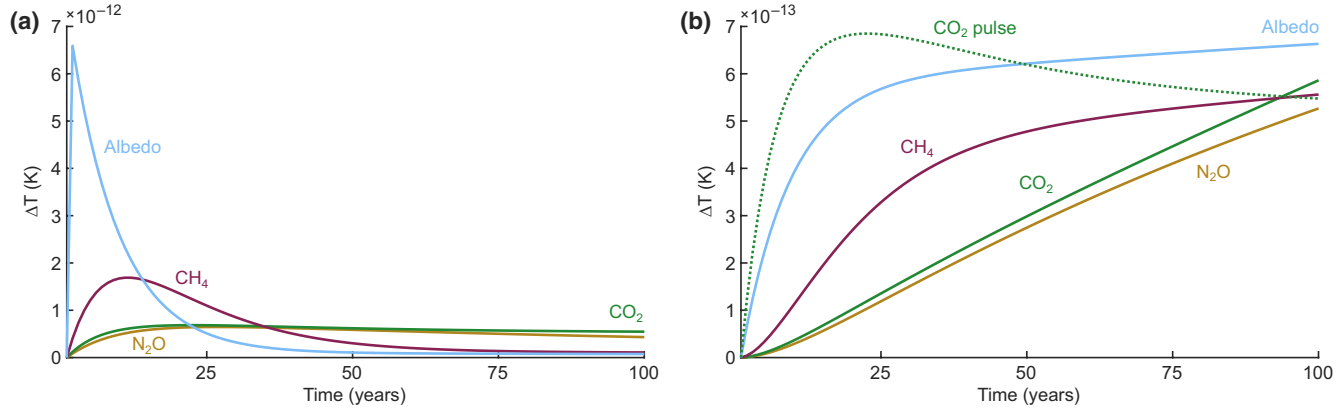

FIGURE 7 Annual temperature response to GWP_{100} of 1 Mg CO_2e resulting from (a) emission pulses of 1 Mg CO_2, 27.8 kg N_2O or 3.4 kg fossil CH_4, or from annual mean albedo RF of 9.2×10^{-11} W/m^2 during 1 year; and (b) from sustained emissions or albedo RF at constant rate over 100 years; the response to the CO_2 pulse is reproduced from (a) for comparison. GWP, global warming potential; RF, radiative forcing. Metric values taken from Myhre et al. (2013)

appears to the evaluation time. In other words, GWP gives the same weight to inventory elements regardless of their timing, whereas $\Delta T[H]$ gives forcings different weights depending on when they appear with respect to H. The weighting over time is specific for each forcing agent and given by its AGTP (see Equations 9–11). Consequently, the same result in terms of GWP_{100} (e.g. 1 kg CO_2e) can imply substantially different temperature responses over time depending on (a) the perturbation lifetime and decay timescales of the climate forcers involved (Figure 7); and (b) the distribution of emissions and albedo RF throughout the study period. For reason (a), albedo RF in years 1–49 was relatively more important for the climate impact using GWP_{100} than using $\Delta T[100]$. For reason (b), temporary carbon storage in biomass was 'climate neutral' with GWP_{100}, but gave a cooling or warming temperature response at different points in time (see Table 2).

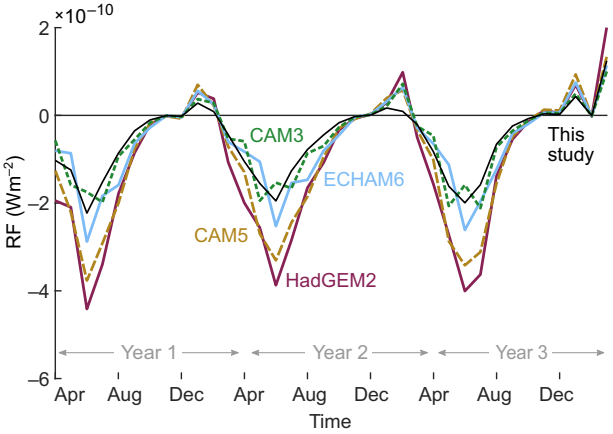

FIGURE 8 Monthly radiative forcing (RF) from albedo change during a 3-year cutting cycle of willow, calculated using monthly radiative kernels from global climate models; albedo RF using the method in this study with 5-day resolution is shown for comparison

3.3 | Sensitivity analysis

A 20% reduction in yields mainly affected the result of the willow scenario due to lower soil carbon sequestration (0.59 Mg C ha^{-1} year^{-1} on average during the study period, i.e. −30% compared with the baseline). Yield-induced changes in biomass carbon stocks, production chain (e.g. harvesting, transport and combustion) and N_2O emissions from soil had smaller effects on the results. In total, the cooling effect of the willow system was reduced by 55% using $\Delta T[100]$ per hectare and by 29% using GWP_{100} per MJ fuel. The reference scenario was primarily affected due to reduced demand for natural gas, resulting in 17% lower climate impact with $\Delta T[100]$ per hectare (Table S12, including figures).

A 20% reduction in initial soil carbon stocks led to a higher net gain in the willow scenario (0.91 Mg C ha^{-1} year^{-1} on average during the study period, i.e. +10% compared with the baseline). The cooling effect of the willow scenario increased by 22% using $\Delta T[100]$ per hectare and by 17% using GWP_{100} per MJ fuel (Table S12). The net gain was a result of smaller losses from the initial soil carbon stock, while the inputs from plant residues remained the same as in the baseline. Consequently, the absolute difference to the baseline was almost identical in both scenarios. A slightly higher loss of initial soil carbon under fallow was due to higher decomposer activity (see Equations 1 and 2).

Using an alternative site as a proxy for the albedo of fallow (0.184), smaller albedo change in the willow scenario resulted in 36% lower RF on average over each cutting cycle (Table S11). The GWP_{100} and the temperature response scaled linearly to RF.

Using monthly radiative kernels from CAM3, ECHAM6, CAM6 and HadGEM2 to calculate RF from albedo change

in the willow scenario resulted in 2%, 15%, 78% and 100% higher albedo RF on average over the cutting cycle, respectively, compared with the method used in this study with 5 day resolution (Table S13b). The kernels from global climate models were higher in most months than the equivalent calculated with our data (Table S13a). Consequently, albedo RF was more strongly negative in summer and more strongly positive in winter in every year of the cutting cycle (Figure 8).

4 | DISCUSSION

4.1 | Climate impact of willow bioenergy

A net cooling effect of SRC willow bioenergy was found in terms of global mean surface temperature change per hectare (-10.1×10^{-11} K in year 50, -3.8×10^{-11} K in year 100) and GWP_{100} per MJ fuel energy content (−12.2 g CO_2e), even when replacement of fossil fuels was not considered. The main cooling in the willow scenario was a result of soil carbon sequestration, thanks to high inputs of carbon from root and leaf biomass. Soil carbon stock change was sensitive to yield levels and may be lower or potentially negative on land with high initial carbon stocks (Hillier et al., 2009). Net carbon sequestration relative to the reference land use was positive and not affected by the initial carbon stock. Our findings are consistent with yields, carbon sequestration, soil N_2O and life cycle GHG emissions reported elsewhere for SRC cultivated on former cropland (as opposed to native vegetation or perennial grasslands; Creutzig et al., 2015; Don et al., 2012; Whitaker et al., 2018). The SRC willow system has been shown to be carbon-negative despite uncertainties associated with management and biological parameters such as yield, litterfall and soil carbon sequestration (Caputo et al., 2014).

Natural gas in the reference scenario was the single largest source of emissions and thus substitution of this fossil fuel gave the greatest potential for climate change mitigation in the case study. Substituting bioenergy for natural gas over the production period could avoid a maximum warming of 38.4×10^{-11} K/ha in year 56, or emissions of 79.9 g CO_2e/MJ fuel, adding to the climate change mitigation potential of the willow scenario alone.

Albedo increased under willow relative to the former fallow and hence contributed to the cooling effect. Albedo RF accounted for 34% of GWP_{100}, 36% of $\Delta T[50]$ and 6% of $\Delta T[100]$ in the willow scenario. The albedo effect dominated on short timescales of 10–20 years and offset the warming from production chain emissions during the study period. Its relative importance decreased over time, owing to accumulation of soil carbon under sustained production (a property of the chosen scenario) and the longer perturbation lifetime of GHGs (a property of the climate system). This relationship would be the reverse in a scenario of permanent land use change where soil carbon stocks have reached a new equilibrium. Sustained albedo change leads to constant RF and a stabilizing temperature response, whereas the effect of elevated yet stable soil carbon stocks decays according to the removal rate of CO_2 from the atmosphere. This difference can be observed in the willow scenario by comparing the effect of albedo change and elevated yet stable biomass carbon stocks under sustained production (see Figure 6a).

4.2 | Importance of albedo and uncertainties

The results demonstrated the potential importance of albedo change for the life cycle climate impact of bioenergy from SRC willow. The relative importance of albedo change as a climate forcer varies over time and depends on case-specific factors such as local climate, insolation, soil type, management, yield, reference land use and study period duration. Understanding the potential magnitude of the albedo effect can help decide whether to include albedo in future assessments of bioenergy. Once fossil fuel emissions have been cut, the next challenge is to mitigate impacts of bioenergy feedstock production and to foster potential climate benefits by carbon sequestration and higher albedo. Willow as a perennial energy crop is known for low emissions from feedstock production and high carbon sequestration potential (Don et al., 2012). Annual energy crops are more resource-intensive and usually reduce soil carbon stocks (Hillier et al., 2009), so albedo change could act as an important cooling factor in annual cropping systems, especially in regions with higher solar irradiance than in Sweden (Cai et al., 2016; Caiazzo et al., 2014).

Albedo of the reference land use was an important variable in the assessment. Albedo is often considered per land cover type, although there can be substantial variation. Ranges of 0.16–0.26 have been reported for grassland and 0.15–0.20 for deciduous forest (Bonan, 2015). Assuming grass as a proxy for green fallow and deciduous trees as a proxy for SRC willow, a warming effect could be expected from albedo change in our scenario, and a cooling effect from any reduction in tree cover. Indeed, albedo RF of 0 to -0.71×10^{-11} W m^{-2} ha^{-1} has been found for generic (non-species specific) conversion of woody vegetation (forest and shrubland) to non-woody vegetation (crops and grassland) in different world regions (Jones, Calvin, Collins, & Edmonds, 2015), although that study also included non-radiative effects. Our data and other studies suggest that SRC willow is more reflective than most broadleaf species (Levy, Burakowski, & Richardson, 2018), and that the vegetation typically found on fallow land has lower albedo than productive and potentially fertilized grasslands (Hollinger et al., 2010). Moreover, we found smaller effects due to reduced snow cover than suggested by global modelling studies on shifting grassland to forest in the

northern mid-latitudes (Arora & Montenegro, 2011; Betts, 2000), confirming similar findings for a plantation of hybrid poplar (Cai, Price, Orchansky, & Thomas, 2011).

Albedo RF calculated with the isotropic single-layer radiative transfer model was lower than that obtained with monthly radiative kernels mimicking sophisticated radiative transfer schemes, indicating that our model underestimated upward transmittance of reflected radiation through the atmosphere. However, the spread of the four sets of kernels considered was larger than the difference between the lowest kernels and our values. The kernels are associated with other uncertainties, for example, the atmospheric state climatology of a climate model might not be representative of current conditions (Bright & O'Halloran, 2019) or interactions between albedo and clouds on submonthly timescales may be omitted (Soden et al., 2008).

Climate sensitivity to albedo RF relative to CO_2 forcing is a remaining source of uncertainty. The literature is inconclusive, suggesting that RF from land cover change may have a weaker or stronger effect on global mean surface temperature change than the same amount of CO_2 forcing. Values of 0.50, 0.78, 0.79 and 1.02 for $\lambda_\alpha/\lambda_{CO_2}$ have been estimated for global-scale land use change based on experiments with different climate models (Davin & de Noblet-Ducoudré, 2010; Davin, de Noblet-Ducoudré, & Friedlingstein, 2007; Hansen et al., 2005; Jones, Collins, & Torn, 2013). The variation stems from factors related to the model used (parameterization, processes and feedbacks included) and the experiment performed (vegetation types and surface variables modified jointly with albedo; Bright et al., 2015). Laguë, Bonan, and Swann (2019) disentangled temperature effects by surface variable (albedo, evaporative resistance and surface roughness) and mechanism (surface effects and atmospheric feedbacks). However, applying an efficacy factor on albedo RF may still not result in the same global temperature change as an equivalent amount of CO_2 forcing, a limitation of the RF concept in capturing land use change effects (Jones et al., 2013).

4.3 | Climate metrics for albedo

The timing of emissions and forcings was reflected in the results for the time-dependent metric ΔT, but not for GWP_{100} (Ericsson et al., 2013). GWP_{100} was easy to use once albedo change had been converted to RF using a (simplified) radiative transfer model, but it obscured that only 1% of the initial temperature effect of albedo change lasts for 100 years (see Equation 11). GWP_{100} is frequently used to express albedo RF in carbon or CO_2 equivalents to make it comparable to the impact of GHGs (Betts, 2000; Caiazzo et al., 2014; Cherubini et al., 2012; Muñoz, Campra, & Fernández-Alba, 2010; Schwaiger & Bird, 2010; Zhao & Jackson, 2014). We developed a theoretical GWP_{100} characterization factor for albedo RF (10.9×10^{12} kg CO_2e $(W\ m^{-2})^{-1}$) and demonstrated that using it as a time-independent metric can bias LCA results.

When using GWP_{100}, the climate change mitigation potential of temporary carbon storage was overlooked and the importance of albedo relative to CO_2 was understated on short timescales and overstated on timescales longer than 22 years after emission or albedo change. This agrees with previous findings that GWP_{100} effectively measures the relative impact of long-lived and short-lived pollutants on temperatures 20–40 years after emission and thus overstates the role of cutting current emissions of short-lived pollutants if the goal is to limit peak warming (Allen et al., 2016). This was shown to be also true for albedo in our study, with GWP_{100} indicating the temperature impact of an equivalent CO_2 pulse 22 and 50 years after emission, under temporary and sustained albedo change respectively (see Figure 7). A similar observation has been made for afforestation, where the short- to medium-term nature of the albedo effect (here warming) might hamper the option to 'buy time' until transformations in the energy sector come into effect (Schaeffer et al., 2006). Including the timing of impacts in LCA results can significantly improve their relevance to climate targets, since albedo change and GHGs act on different timescales.

4.4 | Areas of application

The method presented in this study can be used to estimate the effect of albedo change on the global climate and relate it to that of GHG emissions in LCA. It includes first-order radiative effects of albedo change, but not the fate of the absorbed energy in latent heat, sensible heat and outgoing longwave radiation. Moreover, changes in evapotranspiration efficiency and aerodynamic roughness are not considered. These initially non-radiative processes can lead to atmospheric feedbacks that affect shortwave or longwave fluxes locally or remotely (Devaraju, de Noblet-Ducoudré, Quesada, & Bala, 2018; Laguë et al., 2019). In terms of their effect on surface temperature, non-radiative processes are reported to be comparable in magnitude and opposite in sign to radiative processes (Burakowski et al., 2018). However, capturing such processes requires complex climate models, which are less suited to answer the questions usually dealt with in LCA studies. In temperate regions where radiative processes dominate the land cover change effects, the RF concept can be acceptable to quantify impacts on the global climate (Davin & de Noblet-Ducoudré, 2010; Pielke et al., 2002).

There is still a need for methods to account for the climate impact of land use in a comprehensive manner (Bernier et al., 2011). Different methods have been used for local effects, but for global climate impacts comparable

to GHGs there are few alternatives to RF (Bright et al., 2015). In this study we demonstrated how to quantify the magnitude and uncertainties of the albedo effect in LCA in relation to that of GHGs emitted along the supply chain of bioenergy and compared the climate impact of bioenergy due to albedo and GHGs with that of alternative energy sources and land uses.

ACKNOWLEDGEMENTS

This work was supported by the Swedish strategic research programme STandUP for Energy. The authors thank Per Weslien (University of Gothenburg) and Patrik Vestin (Lund University) for providing radiation data and site information, and Martin Bolinder (Dept. of Ecology, SLU) for contributing expertise on soil carbon modelling.

ORCID

Petra Sieber https://orcid.org/0000-0003-2626-9502
Niclas Ericsson https://orcid.org/0000-0002-3057-1563
Torun Hammar https://orcid.org/0000-0003-2961-5933

REFERENCES

Aamaas, B., Berntsen, T. K., Fuglestvedt, J. S., Shine, K. P., & Bellouin, N. (2016). Regional emission metrics for short-lived climate forcers from multiple models. *Atmospheric Chemistry and Physics*, *16*(11), 7451–7468. https://doi.org/10.5194/acp-16-7451-2016

Aamaas, B., Peters, G. P., & Fuglestvedt, J. S. (2013). Simple emission metrics for climate impacts. *Earth System Dynamics*, *4*(1), 145–170. https://doi.org/10.5194/esd-4-145-2013

Akbari, H., Menon, S., & Rosenfeld, A. (2009). Global cooling: Increasing world-wide urban albedos to offset CO_2. *Climatic Change*, *94*(3–4), 275–286. https://doi.org/10.1007/s10584-008-9515-9

Allen, M. R., Fuglestvedt, J. S., Shine, K. P., Reisinger, A., Pierrehumbert, R. T., & Forster, P. M. (2016). New use of global warming potentials to compare cumulative and short-lived climate pollutants. *Nature Climate Change*, *6*(8), 773–776. https://doi.org/10.1038/nclimate2998

Andrén, O., & Kätterer, T. (1997). ICBM: The introductory carbon balance model for exploration of soil carbon balances. *Ecological Applications*, *7*(4), 1226–1236. https://doi.org/10.1890/1051-0761(1997)007[1226:ITICBM]2.0.CO;2

Andrén, O., Kätterer, T., & Karlsson, T. (2004). ICBM regional model for estimations of dynamics of agricultural soil carbon pools. *Nutrient Cycling in Agroecosystems*, *70*(2), 231–239. https://doi.org/10.1023/B:FRES.0000048471.59164.ff

Aronsson, P., Rosenqvist, H., & Dimitriou, I. (2014). Impact of nitrogen fertilization to short-rotation willow coppice plantations grown in Sweden on yield and economy. *BioEnergy Research*, *7*(3), 993–1001. https://doi.org/10.1007/s12155-014-9435-7

Arora, V. K., & Montenegro, A. (2011). Small temperature benefits provided by realistic afforestation efforts. *Nature Geoscience*, *4*, 514–518. https://doi.org/10.1038/ngeo1182

Arvesen, A., Cherubini, F., del Alamo Serrano, G., Astrup, R., Becidan, M., Belbo, H., … Strømman, A. H. (2018). Cooling aerosols and changes in albedo counteract warming from CO_2 and black carbon from forest bioenergy in Norway. *Scientific Reports*, *8*(1), 3299. https://doi.org/10.1038/s41598-018-21559-8

Bernier, P. Y., Desjardins, R. L., Karimi-Zindashty, Y., Worth, D., Beaudoin, A., Luo, Y., & Wang, S. (2011). Boreal lichen woodlands: A possible negative feedback to climate change in eastern North America. *Agricultural and Forest Meteorology*, *151*(4), 521–528. https://doi.org/10.1016/j.agrformet.2010.12.013

Betts, R. A. (2000). Offset of the potential carbon sink from boreal forestation by decreases in surface albedo. *Nature*, *408*(6809), 187–190. https://doi.org/10.1038/35041545

Betts, R. A., Falloon, P. D., Goldewijk, K. K., & Ramankutty, N. (2007). Biogeophysical effects of land use on climate: Model simulations of radiative forcing and large-scale temperature change. *Agricultural and Forest Meteorology*, *142*(2–4), 216–233. https://doi.org/10.1016/j.agrformet.2006.08.021

Bolinder, M. A., Janzen, H. H., Gregorich, E. G., Angers, D. A., & VandenBygaart, A. J. (2007). An approach for estimating net primary productivity and annual carbon inputs to soil for common agricultural crops in Canada. *Agriculture, Ecosystems & Environment*, *118*(1), 29–42. https://doi.org/10.1016/j.agee.2006.05.013

Bonan, G. (2015). *Ecological climatology: Concepts and applications* (3rd ed.). Cambridge, UK: Cambridge University Press.

Börjesson, P. (2006). Livscykelanalys av Salixproduktion (Life cycle assessment of willow production) (Vol. 60). IMES/EESS report. Lund, Sweden: Department of Environmental and Energy Systems Studies, Lund University.

Boucher, O., & Reddy, M. S. (2008). Climate trade-off between black carbon and carbon dioxide emissions. *Energy Policy*, *36*(1), 193–200. https://doi.org/10.1016/j.enpol.2007.08.039

Bright, R. M., & O'Halloran, T. L. (2019). Developing a monthly radiative kernel for surface albedo change from satellite climatologies of Earth's shortwave radiation budget: CACK v1.0. *Geoscientific Model Development*, *12*(9), 3975–3990. https://doi.org/10.5194/gmd-12-3975-2019

Bright, R. M., Stromman, A. H., & Peters, G. P. (2011). Radiative forcing impacts of boreal forest biofuels: A scenario study for Norway in light of albedo. *Environmental Science & Technology*, *45*(17), 7570–7580. https://doi.org/10.1021/es201746b

Bright, R. M., Zhao, K. G., Jackson, R. B., & Cherubini, F. (2015). Quantifying surface albedo and other direct biogeophysical climate forcings of forestry activities. *Global Change Biology*, *21*(9), 3246–3266. https://doi.org/10.1111/gcb.12951

Burakowski, E., Tawfik, A., Ouimette, A., Lepine, L., Novick, K., Ollinger, S., … Bonan, G. (2018). The role of surface roughness, albedo, and Bowen ratio on ecosystem energy balance in the Eastern United States. *Agricultural and Forest Meteorology*, *249*, 367–376. https://doi.org/10.1016/j.agrformet.2017.11.030

Cai, H., Wang, J., Feng, Y., Wang, M., Qin, Z., & Dunn, J. B. (2016). Consideration of land use change-induced surface albedo effects in life-cycle analysis of biofuels. *Energy & Environmental Science*, *9*(9), 2855–2867. https://doi.org/10.1039/c6ee01728b

Cai, T., Price, D. T., Orchansky, A. L., & Thomas, B. R. (2011). Carbon, water, and energy exchanges of a hybrid poplar plantation during the first five years following planting. *Ecosystems*, *14*(4), 658–671. https://doi.org/10.1007/s10021-011-9436-8

Caiazzo, F., Malina, R., Staples, M. D., Wolfe, P. J., Yim, S. H. L., & Barrett, S. R. H. (2014). Quantifying the climate impacts of albedo changes due to biofuel production: A comparison with biogeochemical effects. *Environmental Research Letters*, *9*(2), 024015. https://doi.org/10.1088/1748-9326/9/2/024015

Caputo, J., Balogh, S. B., Volk, T. A., Johnson, L., Puettmann, M., Lippke, B., & Oneil, E. (2014). Incorporating uncertainty into a life

cycle assessment (LCA) model of short-rotation willow biomass (*Salix* spp.) crops. *BioEnergy Research*, *7*(1), 48–59. https://doi.org/10.1007/s12155-013-9347-y

Carrer, D., Pique, G., Ferlicoq, M., Ceamanos, X., & Ceschia, E. (2018). What is the potential of cropland albedo management in the fight against global warming? A case study based on the use of cover crops. *Environmental Research Letters*, *13*(4), 044030. https://doi.org/10.1088/1748-9326/aab650

Cherubini, F., Bird, N. D., Cowie, A., Jungmeier, G., Schlamadinger, B., & Woess-Gallasch, S. (2009). Energy- and greenhouse gas-based LCA of biofuel and bioenergy systems: Key issues, ranges and recommendations. *Resources Conservation and Recycling*, *53*(8), 434–447. https://doi.org/10.1016/j.resconrec.2009.03.013

Cherubini, F., Bright, R. M., & Stromman, A. H. (2012). Site-specific global warming potentials of biogenic CO_2 for bioenergy: Contributions from carbon fluxes and albedo dynamics. *Environmental Research Letters*, *7*(4). https://doi.org/10.1088/1748-9326/7/4/045902

Copernicus Climate Change Service (C3S). (2017). *ERA5: Fifth generation of ECMWF atmospheric reanalyses of the global climate*. Retrieved from https://cds.climate.copernicus.eu/

Creutzig, F., Ravindranath, N. H., Berndes, G., Bolwig, S., Bright, R., Cherubini, F., … Masera, O. (2015). Bioenergy and climate change mitigation: An assessment. *GCB Bioenergy*, *7*(5), 916–944. https://doi.org/10.1111/gcbb.12205

Davin, E. L., & de Noblet-Ducoudré, N. (2010). Climatic impact of global-scale deforestation: Radiative versus nonradiative processes. *Journal of Climate*, *23*(1), 97–112. https://doi.org/10.1175/2009JCLI3102.1

Davin, E. L., de Noblet-Ducoudré, N., & Friedlingstein, P. (2007). Impact of land cover change on surface climate: Relevance of the radiative forcing concept. *Geophysical Research Letters*, *34*(13). https://doi.org/10.1029/2007gl029678

de Ruijter, F. J., & Huijsmans, J. F. M. (2012). *Ammonia emissions from crop residues*. Wageningen, The Netherlands: Plant Reserach International, Wageningen University and Reserach.

Devaraju, N., de Noblet-Ducoudré, N., Quesada, B., & Bala, G. (2018). Quantifying the relative importance of direct and indirect biophysical effects of deforestation on surface temperature and teleconnections. *Journal of Climate*, *31*(10), 3811–3829. https://doi.org/10.1175/jcli-d-17-0563.1

Don, A., Osborne, B., Hastings, A., Skiba, U., Carter, M. S., Drewer, J., … Zenone, T. (2012). Land-use change to bioenergy production in Europe: Implications for the greenhouse gas balance and soil carbon. *GCB Bioenergy*, *4*(4), 372–391. https://doi.org/10.1111/j.1757-1707.2011.01116.x

Elinder, M., Almquist, A., & Jirjis, R. (1995). *Kyllagring av salixflis ventilerad med kall uteluft (Cold air ventilated storage of Salix chips)*. SLF report 18. Stockholm, Sweden: Stiftelsen Lantbruksforskning.

Ericsson, N., Porsö, C., Ahlgren, S., Nordberg, A., Sundberg, C., & Hansson, P.-A. (2013). Time-dependent climate impact of a bioenergy system – Methodology development and application to Swedish conditions. *GCB Bioenergy*, *5*(5), 580–590. https://doi.org/10.1111/gcbb.12031

Fuglestvedt, J. S., Shine, K. P., Berntsen, T., Cook, J., Lee, D. S., Stenke, A., … Waitz, I. A. (2010). Transport impacts on atmosphere and climate: Metrics. *Atmospheric Environment*, *44*(37), 4648–4677. https://doi.org/10.1016/j.atmosenv.2009.04.044

Gelfand, I., Sahajpal, R., Zhang, X., Izaurralde, R. C., Gross, K. L., & Robertson, G. P. (2013). Sustainable bioenergy production from marginal lands in the US Midwest. *Nature*, *493*(7433), 514–517. https://doi.org/10.1038/nature11811

Ghimire, B., Williams, C. A., Masek, J., Gao, F., Wang, Z., Schaaf, C., & He, T. (2014). Global albedo change and radiative cooling from anthropogenic land cover change, 1700 to 2005 based on MODIS, land use harmonization, radiative kernels, and reanalysis. *Geophysical Research Letters*, *41*(24), 9087–9096. https://doi.org/10.1002/2014GL061671

Hammar, T., Ericsson, N., Sundberg, C., & Hansson, P.-A. (2014). Climate impact of willow grown for bioenergy in Sweden. *BioEnergy Research*, *7*(4), 1529–1540. https://doi.org/10.1007/s12155-014-9490-0

Hammar, T., Hansson, P.-A., & Sundberg, C. (2017). Climate impact assessment of willow energy from a landscape perspective: A Swedish case study. *GCB Bioenergy*, *9*(5), 973–985. https://doi.org/10.1111/gcbb.12399

Hansen, J., Sato, M., Ruedy, R., Nazarenko, L., Lacis, A., Schmidt, G. A., … Zhang, S. (2005). Efficacy of climate forcings. *Journal of Geophysical Research: Atmospheres*, *110*(D18). https://doi.org/10.1029/2005JD005776

Heller, M. C., Keoleian, G. A., & Volk, T. A. (2003). Life cycle assessment of a willow bioenergy cropping system. *Biomass and Bioenergy*, *25*(2), 147–165. https://doi.org/10.1016/S0961-9534(02)00190-3

Hellweg, S., & Milà i Canals, L. (2014). Emerging approaches, challenges and opportunities in life cycle assessment. *Science*, *344*(6188), 1109–1113. https://doi.org/10.1126/science.1248361

Hillier, J., Whittaker, C., Dailey, G., Aylott, M., Casella, E., Richter, G. M., … Smith, P. (2009). Greenhouse gas emissions from four bioenergy crops in England and Wales: Integrating spatial estimates of yield and soil carbon balance in life cycle analyses. *Global Change Biology Bioenergy*, *1*(4), 267–281. https://doi.org/10.1111/j.1757-1707.2009.01021.x

Hollinger, D. Y., Ollinger, S. V., Richardson, A. D., Meyers, T. P., Dail, D. B., Martin, M. E., … Verma, S. B. (2010). Albedo estimates for land surface models and support for a new paradigm based on foliage nitrogen concentration. *Global Change Biology*, *16*(2), 696–710. https://doi.org/10.1111/j.1365-2486.2009.02028.x

Hollsten, R., Arkelöv, O., & Ingelman, G. (2013). *Handbok för salixodlare (Manual for willow farmers)* (2nd ed.). Jönköping, Sweden: Swedish Board of Agriculture.

IPCC. (2019). *2019 Refinement to the 2006 IPCC Guidelines for National Greenhouse Gas Inventories*. Hayama, Japan: IGES.

Jones, A. D., Calvin, K. V., Collins, W. D., & Edmonds, J. (2015). Accounting for radiative forcing from albedo change in future global land-use scenarios. *Climatic Change*, *131*(4), 691–703. https://doi.org/10.1007/s10584-015-1411-5

Jones, A. D., Collins, W. D., & Torn, M. S. (2013). On the additivity of radiative forcing between land use change and greenhouse gases. *Geophysical Research Letters*, *40*(15), 4036–4041. https://doi.org/10.1002/grl.50754

Joos, F., Roth, R., Fuglestvedt, J. S., Peters, G. P., Enting, I. G., von Bloh, W., … Weaver, A. J. (2013). Carbon dioxide and climate impulse response functions for the computation of greenhouse gas metrics: A multi-model analysis. *Atmospheric Chemistry and Physics*, *13*(5), 2793–2825. https://doi.org/10.5194/acp-13-2793-2013

Jørgensen, S. V., Cherubini, F., & Michelsen, O. (2014). Biogenic CO_2 fluxes, changes in surface albedo and biodiversity impacts from establishment of a miscanthus plantation. *Journal of Environmental Management*, *146*, 346–354. https://doi.org/10.1016/j.jenvman.2014.06.033

Kätterer, T., Bolinder, M. A., Andrén, O., Kirchmann, H., & Menichetti, L. (2011). Roots contribute more to refractory soil organic matter than above-ground crop residues, as revealed by a long-term field experiment. *Agriculture, Ecosystems & Environment*, *141*(1), 184–192. https://doi.org/10.1016/j.agee.2011.02.029

Laguë, M. M., Bonan, G. B., & Swann, A. L. S. (2019). Separating the impact of individual land surface properties on the terrestrial surface energy budget in both the coupled and uncoupled land-atmosphere system. *Journal of Climate*, *32*(18), 5725–5744. https://doi.org/10.1175/jcli-d-18-0812.1

Levasseur, A., Cavalett, O., Fuglestvedt, J. S., Gasser, T., Johansson, D. J. A., Jørgensen, S. V., … Cherubini, F. (2016). Enhancing life cycle impact assessment from climate science: Review of recent findings and recommendations for application to LCA. *Ecological Indicators*, *71*, 163–174. https://doi.org/10.1016/j.ecolind.2016.06.049

Levasseur, A., Lesage, P., Margni, M., & Samson, R. (2013). Biogenic carbon and temporary storage addressed with dynamic life cycle assessment. *Journal of Industrial Ecology*, *17*(1), 117–128. https://doi.org/10.1111/j.1530-9290.2012.00503.x

Levy, C. R., Burakowski, E., & Richardson, A. D. (2018). Novel measurements of fine-scale albedo: Using a commercial quadcopter to measure radiation fluxes. *Remote Sensing*, *10*(8), 1303. https://doi.org/10.3390/rs10081303

Meyer, S., Bright, R. M., Fischer, D., Schulz, H., & Glaser, B. (2012). Albedo impact on the suitability of biochar systems to mitigate global warming. *Environmental Science & Technology*, *46*(22), 12726–12734. https://doi.org/10.1021/es302302g

Muñoz, I., Campra, P., & Fernández-Alba, A. R. (2010). Including CO_2-emission equivalence of changes in land surface albedo in life cycle assessment. Methodology and case study on greenhouse agriculture. *The International Journal of Life Cycle Assessment*, *15*(7), 672–681. https://doi.org/10.1007/s11367-010-0202-5

Myhre, G., Shindell, D., Breón, F.-M., Collins, W., Fuglestvedt, J., Huang, J., … Zhang, H. (2013). Anthropogenic and natural radiative forcing supplementary material. In T. F. Stocker, D. Qin, G.-K. Plattner, M. Tignor, S. K. Allen, J. Boschung, A. Nauels, Y. Xia, V. Bex, & P. M. Midgley (Eds.), *Climate change 2013: The physical science basis. Contribution of working group I to the fifth assessment report of the Intergovernmental Panel on Climate Change* (pp. 659–740). Cambridge and New York, NY: Cambridge University Press.

Peters, G. P., Aamaas, B., Lund, M. T., Solli, C., & Fuglestvedt, J. S. (2011). Alternative "global warming" metrics in life cycle assessment: A case study with existing transportation data. *Environmental Science & Technology*, *45*(20), 8633–8641. https://doi.org/10.1021/es200627s

Pielke, R. A., Avissar, R. I., Raupach, M., Dolman, A. J., Zeng, X., & Denning, A. S. (1998). Interactions between the atmosphere and terrestrial ecosystems: Influence on weather and climate. *Global Change Biology*, *4*(5), 461–475. https://doi.org/10.1046/j.1365-2486.1998.t01-1-00176.x

Pielke, R. A., Marland, G., Betts, R. A., Chase, T. N., Eastman, J. L., Niles, J. O., … Running, S. W. (2002). The influence of land-use change and landscape dynamics on the climate system: Relevance to climate-change policy beyond the radiative effect of greenhouse gases. *Philosophical Transactions of the Royal Society of London. Series A: Mathematical, Physical and Engineering Sciences*, *360*(1797), 1705–1719. https://doi.org/10.1098/rsta.2002.1027

Pourhashem, G., Adler, P. R., & Spatari, S. (2016). Time effects of climate change mitigation strategies for second generation biofuels and co-products with temporary carbon storage. *Journal of Cleaner Production*, *112*, 2642–2653. https://doi.org/10.1016/j.jclepro.2015.09.135

Prather, M. J. (2007). Lifetimes and time scales in atmospheric chemistry. *Philosophical Transactions of the Royal Society A: Mathematical, Physical and Engineering Sciences*, *365*(1856), 1705–1726. https://doi.org/10.1098/rsta.2007.2040

Rytter, R.-M. (2001). Biomass production and allocation, including fine-root turnover, and annual N uptake in lysimeter-grown basket willows. *Forest Ecology and Management*, *140*(2), 177–192. https://doi.org/10.1016/S0378-1127(00)00319-4

Schaeffer, M., Eickhout, B., Hoogwijk, M., Strengers, B., Vuuren, D. V., Leemans, R., & Opsteegh, T. (2006). CO_2 and albedo climate impacts of extratropical carbon and biomass plantations. *Global Biogeochemical Cycles*, *20*(2). https://doi.org/10.1029/2005GB002581

Schwaiger, H. P., & Bird, D. N. (2010). Integration of albedo effects caused by land use change into the climate balance: Should we still account in greenhouse gas units? *Forest Ecology and Management*, *260*(3), 278–286. https://doi.org/10.1016/j.foreco.2009.12.002

Searchinger, T., Heimlich, R., Houghton, R. A., Dong, F. X., Elobeid, A., Fabiosa, J., … Yu, T. H. (2008). Use of US croplands for biofuels increases greenhouse gases through emissions from land-use change. *Science*, *319*(5867), 1238–1240. https://doi.org/10.1126/science.1151861

Sieber, P., Ericsson, N., & Hansson, P.-A. (2019). Climate impact of surface albedo change in life cycle assessment: Implications of site and time dependence. *Environmental Impact Assessment Review*, *77*, 191–200. https://doi.org/10.1016/j.eiar.2019.04.003

Smith, P. (2016). Soil carbon sequestration and biochar as negative emission technologies. *Global Change Biology*, *22*(3), 1315–1324. https://doi.org/10.1111/gcb.13178

Soden, B. J., Held, I. M., Colman, R., Shell, K. M., Kiehl, J. T., & Shields, C. A. (2008). Quantifying climate feedbacks using radiative kernels. *Journal of Climate*, *21*(14), 3504–3520. https://doi.org/10.1175/2007jcli2110.1

Statistics Sweden. (2017). *Set-aside (Fallow) 2016 divided by short and long term set-aside*. Retrieved from https://www.scb.se/en/finding-statistics/statistics-by-subject-area/environment/fertilisers-and-lime/use-of-fertilisers-and-animal-manure-and-cultivation-measures-in-agriculture/pong/tables-and-graphs/cultivation-measures/set-aside-fallow-2016-divided-by-short-and-long-term-set-aside/

Stephens, G. L., O'Brien, D., Webster, P. J., Pilewski, P., Kato, S., & Li, J. L. (2015). The albedo of Earth. *Reviews of Geophysics*, *53*(1), 141–163. https://doi.org/10.1002/2014rg000449

Swedish Board of Agriculture. (2019). *Use of agricultural land*. Retrieved from http://www.scb.se/jo0104-en

Tanaka, K., Peters, G. P., & Fuglestvedt, J. S. (2010). Multicomponent climate policy: Why do emission metrics matter? *Carbon Management*, *1*(2), 191–197. https://doi.org/10.4155/cmt.10.28

Tilman, D., Hill, J., & Lehman, C. (2006). Carbon-negative biofuels from low-input high-diversity grassland biomass. *Science*, *314*(5805), 1598–1600. https://doi.org/10.1126/science.1133306

Whitaker, J., Field, J. L., Bernacchi, C. J., Cerri, C. E. P., Ceulemans, R., Davies, C. A., … McNamara, N. P. (2018). Consensus, uncertainties and challenges for perennial bioenergy crops and land use. *GCB Bioenergy*, *10*(3), 150–164. https://doi.org/10.1111/gcbb.12488

Winton, M. (2005). Simple optical models for diagnosing surface-atmosphere shortwave interactions. *Journal of Climate*, *18*(18), 3796–3805. https://doi.org/10.1175/jcli3502.1

Zhao, K., & Jackson, R. B. (2014). Biophysical forcings of land-use changes from potential forestry activities in North America. *Ecological Monographs*, *84*(2), 329–353. https://doi.org/10.1890/12-1705.1

SUPPORTING INFORMATION

Additional supporting information may be found online in the Supporting Information section.

How to cite this article: Sieber P, Ericsson N, Hammar T, Hansson P-A. Including albedo in time-dependent LCA of bioenergy. *GCB Bioenergy*. 2020;12:410–425. https://doi.org/10.1111/gcbb.12682